Experimental Gerontology 142 (2020) 111109

Contents lists available at ScienceDirect

Experimental Gerontology

journal homepage: www.elsevier.com/locate/expgero

# Neuroinflammaging underlies emotional disturbances and circadian rhythm disruption in young male senescence-accelerated mouse prone 8 mice

Naoki Ito[a,*], Hiroaki Takemoto[b,1], Ayana Hasegawa[c], Chika Sugiyama[d], Kengo Honma[d], Takayuki Nagai[a,c,d], Yoshinori Kobayashi[a,b], Hiroshi Odaguchi[a]

[a] Oriental Medicine Research Center, Kitasato University, 5-9-1 Shirokane, Minato-ku, Tokyo 108-8642, Japan
[b] School of Pharmacy, Kitasato University, 5-9-1 Shirokane, Minato-ku, Tokyo 108-8642, Japan
[c] Graduate School of Infection Control Sciences, Kitasato University, 5-9-1 Shirokane, Minato-ku, Tokyo 108-8642, Japan
[d] Laboratory of Biochemical Pharmacology for Phytomedicines, Ōmura Satoshi Memorial Institute, Kitasato University, 5-9-1 Shirokane, Minato-ku, Tokyo 108-8642, Japan

ARTICLE INFO

Section editor: Stephane Baudry

*Keywords:*
Aging
Senescence-accelerated mouse
Neuroinflammation
Microglia
Depression
Circadian rhythm

ABSTRACT

Aging causes psychological dysfunction and neurodegeneration, and can lead to cognitive impairments. Although numerous studies have reported that neurodegeneration and subsequent cognitive impairments are involved in neuroinflammation, relationship between psychological disturbance and neuroinflammation with aging (neuroinflammaging) remains unclear. Here, to clarify the relationship, we examined whether neuroinflammaging affects emotional behaviors in senescence-accelerated mouse prone 8 (SAMP8) mice. Microglial inflammatory responses to a subsequent lipopolysaccharide (LPS) challenge were significantly enhanced in male SAMP8 mice relative to normal aging senescence-accelerated mouse resistant 1 (SAMR1) mice at 17 weeks, but not 8 weeks of age. LPS injection also significantly increased brain and systemic inflammation in SAMP8 mice at 17 weeks. In a battery of behavioral tests, SAMP8 mice at 17 weeks, but not 8 weeks, exhibited anxiety- and depression-like behaviors and circadian rhythm disruption. Taken together, SAMP8 mice at 17 weeks possess a brain microenvironment in which it is easier to trigger neuroinflammatory priming; this may lead to an emergence of anxiety- and depression-like behaviors and circadian rhythm disruption. These findings provide new insights into the temporal relationship between neuroinflammaging and emotion.

## 1. Introduction

Senescence is driven by cellular and molecular levels of damage such as telomere erosion, deoxyribonucleic acid (DNA) damage, epigenetic dysregulation, and mitochondrial dysfunction with aging (Lopez-Otin et al., 2013). Thus, aging and senescence are well documented as risk factors for anorexia (Landi et al., 2016); cancer (de Magalhaes, 2013); diabetes (Gunasekaran and Gannon, 2011); osteoporosis (Zanker and Duque, 2019); cardiovascular disease (Papaconstantinou, 2019); chronic kidney disease (Salimi et al., 2018); neurodegenerative diseases including dementia, Alzheimer's Disease, and Parkinson's Disease (Gambino et al., 2019); mood disorders including depression (Alexopoulos, 2019); and sarcopenia (Dalle et al., 2017). These illnesses are deeply associated with systemic chronic inflammation with aging (Furman et al., 2019), which is called "inflammaging" (Franceschi et al., 2000). Accumulating evidence has also shown that neuroinflammation, indicating low-grade and sterile inflammation in the brain, during aging, named neuroinflammaging (Di Benedetto et al., 2017), plays an important role in neurodegenerative diseases (Pizza et al., 2011). Recently, it was noted that neuroinflammation is closely linked to the pathology of emotional disorders such as depression (Woelfer et al., 2019; Yirmiya et al., 2015). However, the relationship between emotional disorders and neuroinflammaging remains poorly understood.

Senescence-accelerated mouse (SAM) strains originally established from AKR/J mice having phenotypic variations of accelerated aging (Takeda et al., 1981) have been well utilized in the field of neuroinflammation. SAM strains are composed of 2 substrains: SAM prone (SAMP) with a shorter life span (Carter et al., 2005) and SAM resistant (SAMR) with normal aging (Takeda et al., 1997). Among the SAMP

* Corresponding author at: Department of Clinical Research, Oriental Medicine Research Center, Kitasato University, 5-9-1 Shirokane, Minato-ku, Tokyo 108-8642, Japan.
*E-mail address:* ito-n@insti.kitasato-u.ac (N. Ito).
[1] Present address: Faculty of Pharmaceutical Sciences, Toho University, Funabashi, Chiba 274–8510, Japan.

https://doi.org/10.1016/j.exger.2020.111109
Received 17 February 2020; Received in revised form 27 September 2020; Accepted 1 October 2020
Available online 16 October 2020
0531-5565/ 

substrain, SAMP8 mice exhibit age-related impairments in cognitive function (Markowska et al., 1998), emotion (Chen et al., 2007; Meeker et al., 2013), and circadian rhythm (Pang et al., 2006; Sanchez-Barcelo et al., 1997; Yanai and Endo, 2016). Neurobiological and neurochemical studies have also found that SAMP8 mice show increased oxidative stress (Puigoriol-Illamola et al., 2018; Smith et al., 2013), impaired mitochondrial function (Tomobe and Nomura, 2009), amyloid β deposition (Chen et al., 2018; Del Valle et al., 2010), epigenetic alterations (Cosin-Tomas et al., 2014; Grinan-Ferre et al., 2018), and neuroinflammation (Grinan-Ferre et al., 2016; Jiang et al., 2018). Notably, numerous studies have demonstrated a close link between their neurobiological abnormalities, including neuroinflammaging, and cognitive decline in SAMP8 mice at older ages (Diaz-Perdigon et al., 2020; Dong et al., 2018; Jiang et al., 2014; Lin et al., 2014; Yanai et al., 2017; Zhang et al., 2013). However, it remains largely unclear whether neuroinflammaging can affect emotional impairments including depression and anxiety, although some evidence signifies that SAMP8 mice have depression- (Perez-Caceres et al., 2013; Yanai and Endo, 2016) and anxiety-like phenotypes (Chen et al., 2007; Meeker et al., 2013).

In the present study, SAMP8 mice and SAMR1 mice, as a normal aging control strain, were used to examine a potential link between neuroinflammaging and emotional disturbances with aging.

## 2. Materials and methods

### 2.1. Animals

Six-week-old male SAMP8 and SAMR1 mice were purchased from Japan SLC (Hamamatsu, Japan) and allowed to acclimate for at least 1 week after arrival. Mice were housed in a vivarium maintained at a constant temperature (23 ± 2 °C), humidity (55 ± 10%) and a 12-h light/dark cycle (lights on at 08:00) with access to food (CE-2, CLEA Japan, Inc., Tokyo, Japan) and water ad libitum. All cages (22.5 × 33.8 × 14 cm, CLEA Japan, Inc.) were provided with wood bedding material (Japan Laboratory Animals, Inc., Tokyo, Japan). All animal experiments were approved by the Institutional Animal Care and Use Committee of Kitasato University and were performed in accordance with the Guidelines for the Care and Use of Laboratory Animals of Kitasato University and the National Research Council Guide for the Care and Use of Laboratory Animals in Japan. Every effort was made to minimize the number of animals used and their suffering.

### 2.2. Microglia isolation

Microglia were isolated from the whole mouse brain, except the cerebellum, as described previously (Ito et al., 2017; Lee and Tansey, 2013; Singh et al., 2014) with some modifications. For western blot analyses, the cell suspension was centrifuged at 3000 ×*g* for 10 min at 4 °C and the cell pellet was stored at −80 °C until the analysis. For cell cultures, the harvested cells were counted using a handheld automated cell counter (Scepter 2.0; Merck Millipore, Billerica, MA, USA).

### 2.3. Ex vivo microglial stimulation assay with lipopolysaccharide

Microglia were plated at a density of $5 \times 10^4$ cells/well in 96-well plates, kept in a 5% $CO_2$ incubator at 37 °C for 30 min, then stimulated with phosphate-buffered saline (PBS) or *Escherichia coli* lipopolysaccharide (LPS, serotype O111:B4, 0.1 μg/ml; Sigma, St. Louis, MO) for 18 h at 37 °C and 5% $CO_2$. Supernatants were collected and stored at −80 °C until the enzyme-linked immunosorbent assay (ELISA). The remaining cells were incubated with 10% Alamar blue (Thermo Fisher Scientific, Waltham, MA, USA) in DMEM/F12 for 2 h at 37 °C and 5% $CO_2$; cell viability was measured using fluoroscopy with the Infinite M200 microplate reader (Tecan Group Ltd., Männedorf, Switzerland; excitation and emission wavelength: 544 and 590 nm, respectively).

### 2.4. Isolation of brain microvascular endothelial cells

Primary brain microvascular endothelial cells (BMVECs) were isolated from SAMP8 mice aged 8 and 17 weeks as described previously (Banks et al., 2004; Navone et al., 2013; Watanabe et al., 2013) with some modifications. Briefly, following deep isoflurane inhalation to induce anesthesia, mice were decapitated and the whole brain, except the cerebellum, was readily extracted. Meninges from the brain were removed carefully with fine forceps on sterile filter paper (GE Healthcare, Tokyo, Japan). Brains were chopped with fine scissors in ice-cold DMEM (FUJIFILM Wako Pure Chemical Corporation, Osaka, Japan), then digested in a collagenase solution containing collagenase type II (200 U/ml, Worthington Biochemical Corporation) and DNase I (30 U/ml, Sigma) at 37 °C for 30 min. The homogenate was centrifuged at 1000 ×*g* for 20 min at 4 °C in DMEM containing 20% bovine serum albumin (FUJIFILM Wako Pure Chemical Corporation) to remove neurons and glial cells.

The cell pellet was digested again in a solution containing collagenase/dispase (1 mg/ml, Roche Diagnostics, Tokyo, Japan) and DNase I (30 U/ml, Sigma) at 37 °C for 20 min. After centrifugation at 700 ×*g* for 6 min at 4 °C, the cell pellet was resuspended gently in a small amount of DMEM. The cell suspension was added on the top layer of a 33% Percoll Plus gradient (GE Healthcare) and centrifuged at 1000 ×*g* for 10 min at 4 °C. A white layer containing microvessel fragments (Fig. 3A) was carefully collected with a sterile long needle (22G × 70 mm, TERUMO Corporation, Tokyo, Japan) attached to a 5 ml syringe (TERUMO Corporation) and centrifuged at 700 ×*g* for 8 min at 4 °C. The purified microvascular endothelial cells were suspended gently in DMEM/F-12 (Sigma) culture medium supplemented with 20% FBS (Sigma), 1% insulin-transferrin-sodium selenite media supplement (Sigma), 1 mM GlutaMax-I (Thermo Fisher Scientific), 18.5 U/ml heparin (Sigma), 1.5 ng/ml fibroblast growth factor basic (R &D systems, Minneapolis, MN, USA), 1% penicillin/streptomycin (Sigma), 50 μg/ml gentamicin (Sigma), and 4 μg/ml puromycin (Sigma).

BMVECs were seeded in 6-well plates coated with fibronectin (0.1 mg/ml, Sigma) and collagen type IV (0.1 mg/ml, Sigma), then incubated in a 5% $CO_2$ incubator at 37 °C. The medium was changed to culture medium without puromycin every 3 days. At 10 days in vitro (DIV10), the medium was changed, then BMVECs were stimulated with PBS or LPS (serotype O111:B4, 0.01, 0.1, or 1 μg/ml, Sigma) for 24 h at 37 °C and 5% $CO_2$. On DIV11, BMVECs were collected by a cell scraper and stored at −80 °C until the western blot analysis.

### 2.5. Sample collection

After decapitation, brain, blood, and femoral muscle samples were readily collected. The brain was sliced into approximately 1-mm thick coronal sections on dry ice. Blood samples collected in tubes with $K_2$-EDTA (BD, Franklin Lakes, NJ, USA) or Eppendorf tubes (Eppendorf AG, Hamburg, Germany) were centrifuged at 2000 ×*g* for 3 min or twice at 6000 rpm for 1 min at 4 °C for plasma or serum collection, respectively. The samples were stored at −80 °C until assayed.

### 2.6. LPS injection

Mice aged 17 weeks were injected with LPS (0.33 mg/kg) or saline. Intraperitoneal injections were performed at a volume of 10 ml/kg body weight. Twenty-four hours after injection, mice were decapitated, and brain and blood samples were collected. Brain coronal sections and serum were obtained in the same way as described above and stored at −80 °C until western blot analyses and ELISAs were performed.

### 2.7. Western blot

Samples (microglial cells, brain coronal sections [bregma −1.5 to

−2.5 mm], BMVECs, and femoral muscles) were sonicated in lysis buffer (CelLytic™ MT, Sigma) containing 1% (v/v) protease inhibitor cocktail (Sigma) on ice, centrifuged at 18,000 ×*g* for 10 min at 4 °C, and supernatants were collected. The lysate protein concentration was determined by a BCA protein assay kit (Pierce, Rockford, IL, USA). An equal amount of protein (2–3 μg for microglia and BMVECs; 10 μg for brain sections; 5 μg for femoral muscle samples) was loaded into 4–15% sodium dodecyl sulfate polyacrylamide gel electrophoresis (SDS-PAGE; Mini-PROTEAN TGX™ gel, Bio-Rad) and transferred to polyvinylidene difluoride (PVDF) membranes (Bio-Rad) using a Trans-Blot Turbo™ Transfer System (Bio-Rad). The membranes were incubated in blocking buffer (Blocking One solution, Nakalai Tesque, Kyoto, Japan) for 30 min at room temperature (RT). Primary antibodies were diluted in Blocking One solution and membranes were incubated at RT or 4 °C on a shaker (Table S1). After rinsing in Tris buffered saline containing 0.05% (v/v) Tween 20 (TBS-T, Bio-Rad), membranes were incubated with horseradish peroxidase (HRP)-linked anti-rabbit IgG (1:10,000, Cell Signaling Technology, Tokyo, Japan) or HRP-linked anti-goat IgG (1:10,000, Sigma) diluted in TBS-T for 1 h at RT. After rinsing in TBS-T, chemiluminescence was visualized with Clarity Western ECL Substrate or Clarity Max Western ECL Substrate (Bio-Rad) using a ChemiDoc™ Imaging System (ChemiDoc Touch, Bio-Rad). Band intensities were analyzed with ImageLab software (Ver. 6.0, Bio-Rad).

### 2.8. ELISA

Cytokine, steroid, and protein levels in samples were detected using a commercially available ELISA kit for interleukin 6 (IL-6) and IL-1β (BD OptEIA™ ELISA set, BD Biosciences, San Diego, CA, USA), tumor necrosis factor (TNF)-α, IL-4, and IL-10 (Mouse DuoSet ELISA, R&D systems), corticosterone (CORT, AssayMax™ ELISA kit, Assaypro, St. Charles, MO, USA), and troponin-I (Life Diagnostics, West Chester, USA) in accordance with the manufacturers' instructions.

### 2.9. Behavioral tests

Mice were transported to a habituation room and allowed to acclimate to the room for approximately 1 h prior to behavioral testing. All behavioral tests were carried out between 12:00 and 17:00, except for 24-h monitoring with nanotag.

#### 2.9.1. Open field test

Mice were introduced into an opaque grey open field box (40 × 40 × 40 cm) and were allowed to explore freely for 300 s. Time spent in 3 areas (center, between, and periphery), frequency into the center, total distance moved, and total movement were recorded by a video tracking system (EthoVision 3.0; Noldus, Wageningen, Netherlands).

#### 2.9.2. Forced swim test

The forced swim test (FST) was performed as previously described with some modifications (Krishnan et al., 2007). Mice were placed individually into a 5-l beaker containing 4 l of tap water (23 ± 1 °C) for 6 min. A mouse was considered immobile when it ceased struggling and remained floating motionless, only performing the movements necessary to keep its head above water. All behaviors were videotaped and the duration of immobility during the last 4 min of the FST was scored.

#### 2.9.3. Tail suspension test

The tail suspension test (TST) was conducted as previously described with some modifications (Steru et al., 1985). Mice were suspended 50 cm above the floor by their tails, using experimental clips (Yamashitagiken, Tokushima, Japan), to a hook connected to a stainless steel bar for 6 min. The experimental clip was attached approximately 1 cm from the tip of the tail. A mouse was considered immobile only when it ceased struggling and hung motionless. All behaviors were videotaped and the duration of immobility during the last 4 min of the TST was scored.

#### 2.9.4. Sucrose preference test

The sucrose preference test (SPT) was carried out as previously described with some modifications (Liu et al., 2018). Mice were trained to adapt to the presentation of 2 bottles of water in their home cages for 2 days. After adaptation, each mouse had free access to 2 bottles, one containing a 2% sucrose solution and the other containing water, with a counterbalance in its home cage from 17:00 to 9:00. Sucrose preference (SP) was calculated as follows: SP = [2% sucrose solution intake (ml)/ total fluid intake (ml)] x 100.

#### 2.9.5. Twenty-four-hour monitoring of locomotor activity and body temperature

The locomotor activity of mice in their home cages and their body temperatures were simultaneously recorded by a Nanotag sensor (Kissei Comtec Co., Ltd., Nagano, Japan), an implantable three-axis accelerometer and thermometer (weight, 2.6 g; 15 × 14.2 × 7.1 mm). The nanotag was intraperitoneally implanted in mice under inhalation anesthesia. Mice were allowed to recover for at least 1 week. The locomotor activity and body temperature of mice in their home cages were monitored from 8:00 for 24 h and the data were analyzed using the Nanotag viewer program (Kissei Comtec Co., Ltd.).

### 2.10. Statistical analysis

All data are presented as the mean ± the standard error of the mean (SEM) and analyzed using Prism 7 (GraphPad Software, San Diego, CA, USA). For comparisons between 2 groups, statistical analyses were performed using an unpaired *t*-test. For comparisons between 3 or more groups, statistical analysis was performed in experiments for BMVECs, LPS injection, and circadian rhythm using a two-way analysis of variance (ANOVA), followed by a Bonferroni's post hoc test. In all cases, differences were considered statistically significant at $p < 0.05$.

## 3. Results

### 3.1. SAMP8 mice exhibit a brain environment toward neuroinflammatory priming

Under basal culture conditions, there was no difference in IL-6 and IL-1β release into the isolated microglia between SAMR1 and SAMP8 mice aged 8 and 17 weeks. However, IL-6 and IL-1β release from the microglia of SAMP8 mice at 17 weeks, but not 8 weeks, were significantly increased by the LPS challenge compared to that of SAMR1 mice [Fig. 1A; IL-6, $t$ (6) = 3.158, $p = 0.0196$; IL-1β, $t$ (6) = 4.885, $p = 0.0028$]. Protein expression of nod-like receptor family, pyrin domain-containing 3 (NLRP3, a proinflammatory marker) or arginase 1 (Arg1, an anti-inflammatory marker) in microglia derived from the mouse brain at 17 weeks showed no difference between SAMR1 and SAMP8 mice (Fig. 1B and C), but N-type calcium ion channel α1B subunit (Cav2.2) expression was significantly increased in the microglia of SAMP8 mice relative to that of SAMR1 mice [Fig. 1B and C; Cav2.2/GAPDH, $t$ (6) = 3.734, $p = 0.0097$; Cav2.2/Iba1, $t$ (6) = 4.272, $p = 0.0052$].

Under physiological conditions, expression levels of ionized calcium binding adaptor molecule 1 (Iba1, a marker for microglia) and NLRP3 were significantly increased and decreased, respectively, in the brains of SAMP8 mice at 8 weeks relative to that of SAMR1 mice [Fig. 2, left; Iba1/glyceraldehyde 3-phosphate dehydrogenase (GAPDH), $t$ (8) = 2.778, $p = 0.024$; NLRP3/Iba1, $t$ (8) = 3.23, $p = 0.0121$]. At 17 weeks, the expressions of Iba1, Arg1, and intercellular adhesion molecule-1 (ICAM-1, a marker for a cell adhesion molecule) were significantly increased in the brains of SAMP8 mice relative to SAMR1

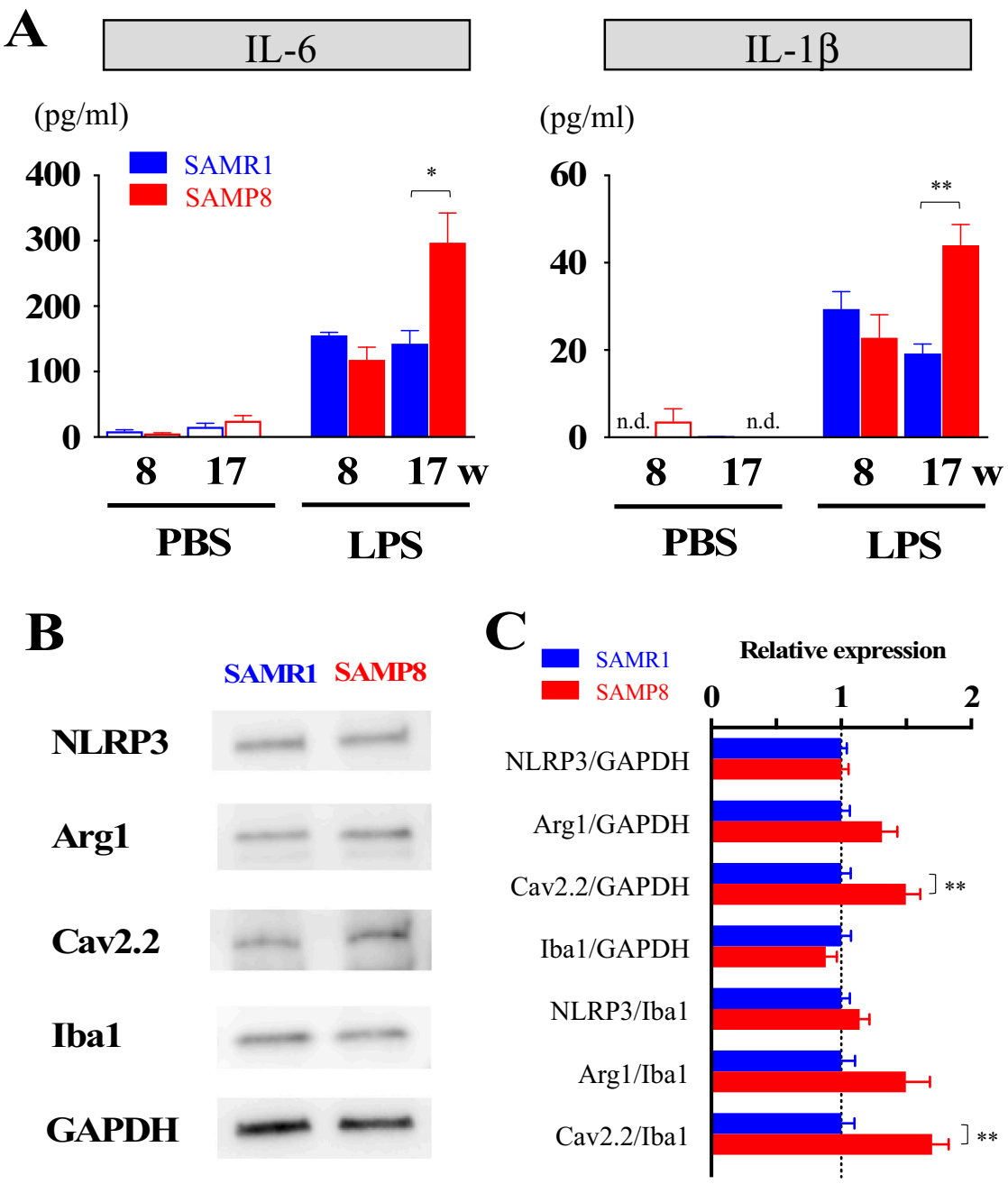


**Fig. 1.** Neuroinflammatory priming in microglia isolated from the brains of SAMP8 mice. (A) IL-6 and IL-1β levels in the supernatant of microglial cultures isolated from mouse brains aged 8 and 17 weeks in the absence or presence of LPS (0.1 μg/ml). (B) Representative western blot images of NLRP3, Arg1, Cav2.2, Iba1, and GAPDH expression in microglial lysates from mice aged 17 weeks. (C) Protein expression levels normalized by GAPDH or Iba1. Data are shown as the mean ± the SEM (A, $n = 3$–4; C, $n = 4$). *$p < 0.05$ and **$p < 0.01$. w, weeks of age.

mice [Fig. 2, right; Iba1/GAPDH, $t$ (18) = 4.332, $p = 0.0004$; Arg1/GAPDH, $t$ (18) = 2.353, $p = 0.0302$; ICAM-1/GAPDH, $t$ (18) = 4.236, $p = 0.0005$]. Moreover, zonula occludens-1 (ZO-1, a marker for tight junction) expression was significantly reduced in the brains of SAMP8 mice relative to SAMR1 mice [Fig. 2, right; ZO-1/GAPDH, $t$ (18) = 3.389, $p = 0.0033$].

In addition, no difference was found in brain cytokine levels between SAMR1 and SAMP8 mice aged either at 8 or 17 weeks, except the TNF-α level in SAMP8 mice was significantly lower than that in 17-week-old SAMR1 mice [Fig. S1, $t$ (16) = 2.781, $p = 0.0134$]. The cumulative CORT level in plasma was significantly higher in SAMP8 mice than in SAMR1 mice [Fig. S2; $t$ (16) = 2.638, $p = 0.0179$]. BMVECs were isolated from the brains of SAMP8 at 8 or 17 weeks, cultured (Fig. 3B), and collected 24 h after an LPS challenge (0–1 ng/ml) for western blot analysis. The addition of LPS induced a dose-dependent increase in cell adhesion molecule expression including ICAM-1 and vascular cell adhesion molecule-1 (VCAM-1) [Fig. 3C, D; two-way ANOVA; ICAM-1; interaction, $F(3,16) = 2.037$, $p = 0.1492$; LPS treatment, $F(3,16) = 77.3$, $p < 0.0001$; age, $F(1,16) = 13.58$, $p = 0.002$: VCAM-1; interaction, $F(3,16) = 3.211$, $p = 0.0512$; LPS treatment, $F(3,16) = 17.6$, $p < 0.0001$; age, $F(1,16) = 16.14$, $p = 0.001$]. The expression when stimulated with LPS (1 ng/ml) was also significantly greater at 17 weeks than 8 weeks (Fig. 3D; Bonferroni's post hoc test; ICAM-1, $p < 0.05$; VCAM-1, $p < 0.05$). A dose-dependent reduction in ZO-1 expression was observed in the cultured BMVECs from SAMP8 mice aged 17 weeks, but not significantly [Fig. 3C, D; two-way ANOVA;

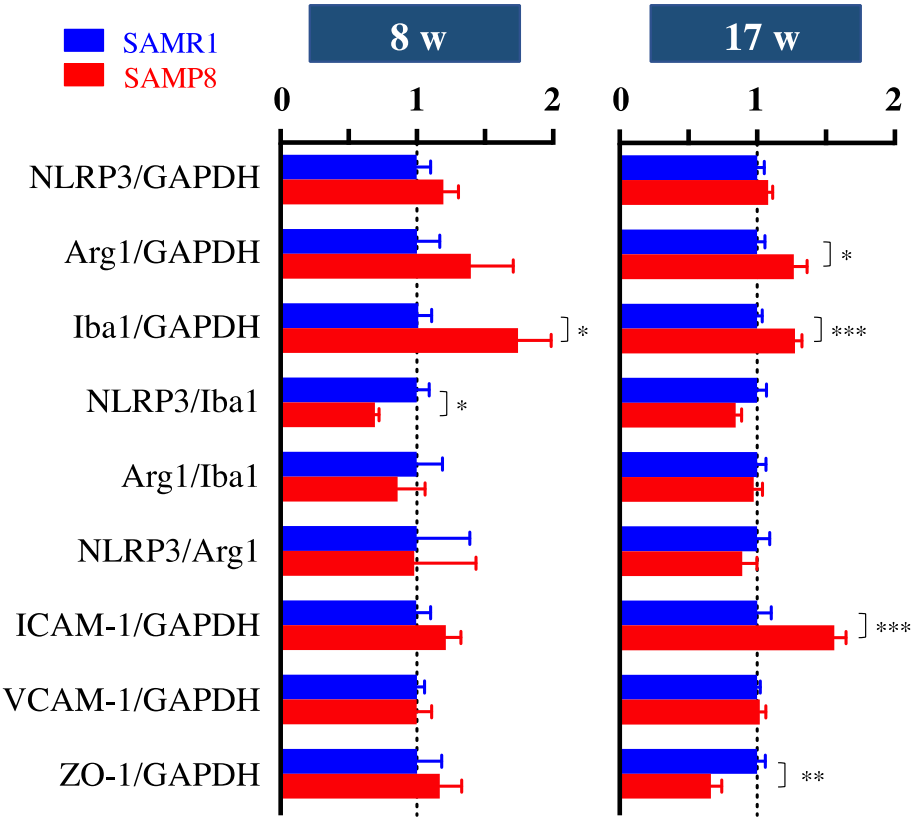


**Fig. 2.** Altered protein expression related to neuroinflammation, cell adhesion molecules, and tight junctions in the brains of SAMP8 mice. Brains were collected from SAMR1 and SAMP8 mice aged 8 and 17 weeks, and then proteins were extracted from coronal brain sections. The relative levels of protein expression related to neuroinflammation, cell adhesion molecules, and tight junctions were examined by western blot and normalized to GAPDH, Iba1, or Arg1. Data are shown as the mean ± the SEM (8 w, $n = 5$; 17 w, $n = 10$). *$p < 0.05$, **$p < 0.01$, and ***$p < 0.001$. w, weeks of age.

interaction, $F(3,16) = 1.21$, $p = 0.3382$; LPS treatment, $F(3,16) = 0.3513$, $p = 0.7887$; age, $F(1,16) = 8.904$, $p = 0.0088$]. BMVEC culture data derived from the SAMR1 mouse brain were not shown in this study, because SAMR1-isolated BMVECs were not able to be cultured under the same cultural conditions as BMVECs from SAMP8 mice.

### 3.2. The neuroinflammation response to lipopolysaccharide is much greater in SAMP8 mice than in SAMR1 mice

In the in vivo experiment, NLRP3 expression in the brains of LPS-injected SAMP8 mice was significantly increased compared to that in LPS-injected SAMR1 mice and saline-injected SAMP8 mice aged 17 weeks [Fig. 4A; two-way ANOVA; interaction, $F(1,12) = 16.26$, $p = 0.0017$; treatment, $F(1,12) = 39.23$, $p < 0.0001$; strain, $F(1,12) = 23.49$, $p = 0.0004$; Bonferroni's post hoc test, $p < 0.001$]. An LPS injection had no effect on Arg1 expression in the brains of SAMR1 or SAMP8 mice (Fig. 4B). LPS injections significantly increased Iba1 expression in the brains of SAMR1 mice relative to saline-injected control [Fig. 4C; two-way ANOVA; interaction, $F(1,12) = 0.9254$, $p = 0.3551$; treatment, $F(1,12) = 24.17$, $p = 0.0004$; strain, $F(1,12) = 4.369$, $p = 0.0586$; Bonferroni's post hoc test, $p < 0.01$]. A ratio of NLRP3 and Arg1 (a balance of pro- and anti-inflammatory phenotypes) significantly increased in LPS-injected SAMP8 mice compared to that in saline-injected controls [Fig. 4D; two-way ANOVA; interaction, $F(1,12) = 1.793$, $p = 0.2054$; treatment, $F(1,12) = 12.86$, $p = 0.0037$; strain, $F(1,12) = 5.051$, $p = 0.0442$; Bonferroni's post hoc test, $p < 0.05$].

LPS injections significantly increased brain ICAM-1 expression in both SAMR1 and SAMP8 mice relative to saline-injected controls [Fig. 4E; two-way ANOVA; interaction, $F(1,12) = 1.943$, $p = 0.1886$; treatment, $F(1,12) = 587.6$, $p < 0.0001$; strain, $F(1,12) = 1.756$, $p = 0.2098$; Bonferroni's post hoc test, $p < 0.001$]. Brain VCAM-1 expression was significantly increased in LPS-injected SAMR1 mice compared to that in saline-injected controls [Fig. 4F; two-way ANOVA; interaction, $F(1,12) = 6.246$, $p = 0.028$; treatment, $F(1,12) = 7.688$, $p = 0.0169$; strain, $F(1,12) = 0.1127$, $p = 0.7429$; Bonferroni's post hoc test, $p < 0.05$]. There was no difference in brain ZO-1 expression between SAMR1 and SAMP8 mice, but a two-way ANOVA revealed a significant reduction in ZO-1 expression by LPS injection [Fig. 4G; interaction, $F(1,12) = 1.515$, $p = 0.242$; treatment, $F(1,12) = 7.37$, $p = 0.0188$; strain, $F(1,12) = 3.354$, $p = 0.092$]. Contrary to the protein expression data in the brain, there was no difference in brain cytokine levels between SAMR1 and SAMP8 mice despite the LPS injection at 17 weeks, except that IL-4 levels in SAMR1 mice were significantly decreased compared to those in saline-injected controls [Fig. S3, two-way ANOVA; interaction, $F(1,12) = 4.869$, $p = 0.0476$; treatment, $F(1,12) = 6.907$, $p = 0.0221$; strain, $F(1,12) = 0.753$, $p = 0.4025$; Bonferroni's post hoc test, $p < 0.05$]. Interestingly, LPS injection markedly increased the serum level of IL-6 in SAMP8 mice compared to that in SAMR1 mice [Fig. 4H; $t(6) = 8.662$, $p < 0.0001$]. Serum IL-1β and TNF-α were not detected in the present experiments (data not shown).

### 3.3. SAMP8 mice show anxiety- and depression-like behaviors with aging

In the OFT under the high light condition (120–130 lx), time spent in the center and between, or in the periphery, was significantly decreased or increased in SAMP8 mice relative to SAMR1 mice aged 17 weeks, respectively [Fig. 5C; Center, $t(24) = 3.561$, $p = 0.0016$; between, $t(24) = 6.118$, $p < 0.0001$; periphery, $t(24) = 5.663$, $p < 0.0001$]. Moreover, a significant low frequency for entering the center area was found in SAMP8 mice relative to SAMR1 mice at 17 weeks [Fig. 5C; $t(24) = 2.143$, $p = 0.0424$]. Movements were also significantly increased in SAMP8 mice relative to SAMR1 mice at 17 weeks [Fig. 5C; $t(24) = 3.633$, $p = 0.0013$]. These results suggest that SAMP8 mice have high anxiety levels at 17 weeks, although no difference was found between SAMR1 and SAMP8 mice at 8 weeks. In addition, under the low light condition (30 lx), significant differences in

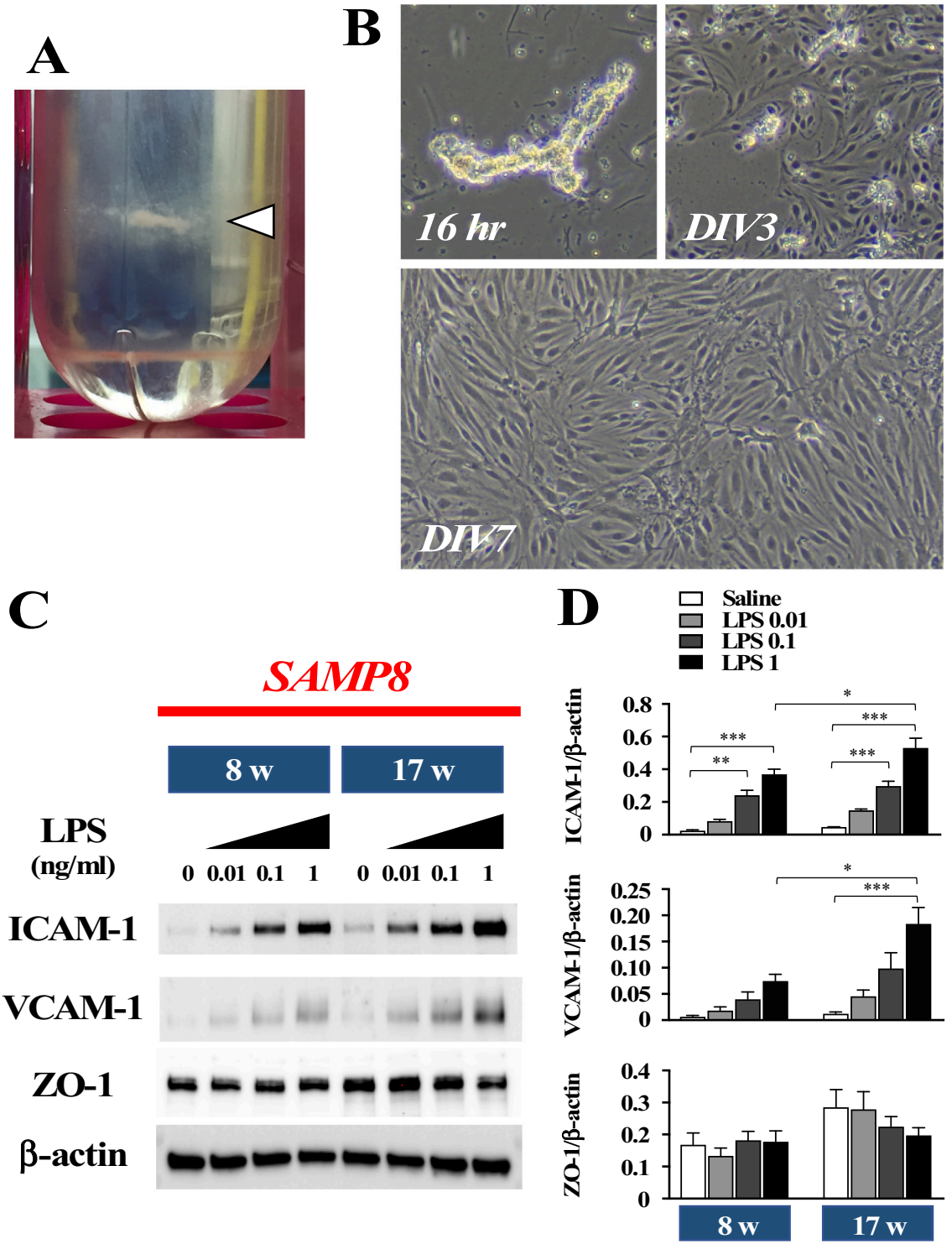


**Fig. 3.** Age related changes in the protein expression of cell adhesion molecules and tight junctions in SAMP8-derived BMVECs when stimulated with LPS. (A) A photo showing a layer containing microvessel fragments (arrowhead) in the Percoll gradient solution. (B) Phase contrast light microscopy images of the SAMP8-derived BMVECs culture at 16 h, DIV3, and DIV7 after seeding. (C) Representative western blot images of adhesion molecules (ICAM-1 and VCAM-1) and tight junction (ZO-1) expression in the BMVECs when stimulated with LPS (0, 0.01, 0.1, and 1 ng/ml). (D) Protein expression levels of ICAM-1, VCAM-1, and ZO-1 normalized by β-actin. Data are shown as the mean ± the SEM ($n = 3$). *$p < 0.05$, **$p < 0.01$, and ***$p < 0.001$. w, weeks of age.

time spent in and the frequency for entering the center that appeared under the high light condition were abolished between SAMR1 and SAMP8 mice at 17 weeks (Fig. S5), suggesting anxiety levels are likely to be attenuated under low light conditions in SAMP8 mice.

In the FST and TST, SAMP8 mice had a significant increase in the total duration of immobility compared to SAMR1 mice at 17 weeks [Fig. 6A, B; FST, $t$ (29) = 4.74, $p < 0.0001$; TST, $t$ (26) = 4.09, $p = 0.0004$]. In the SPT, the SP ratio was also significantly decreased in SAMP8 mice relative to SAMR1 mice at 17 weeks [Fig. 6C; $t$ (14) = 3.207, $p = 0.0063$]. In contrast, there was no change in the immobility or SP between SAMR1 and SAMP8 mice at 8 weeks in either behavioral test. These results suggest that SAMP8 mice aged 17 weeks

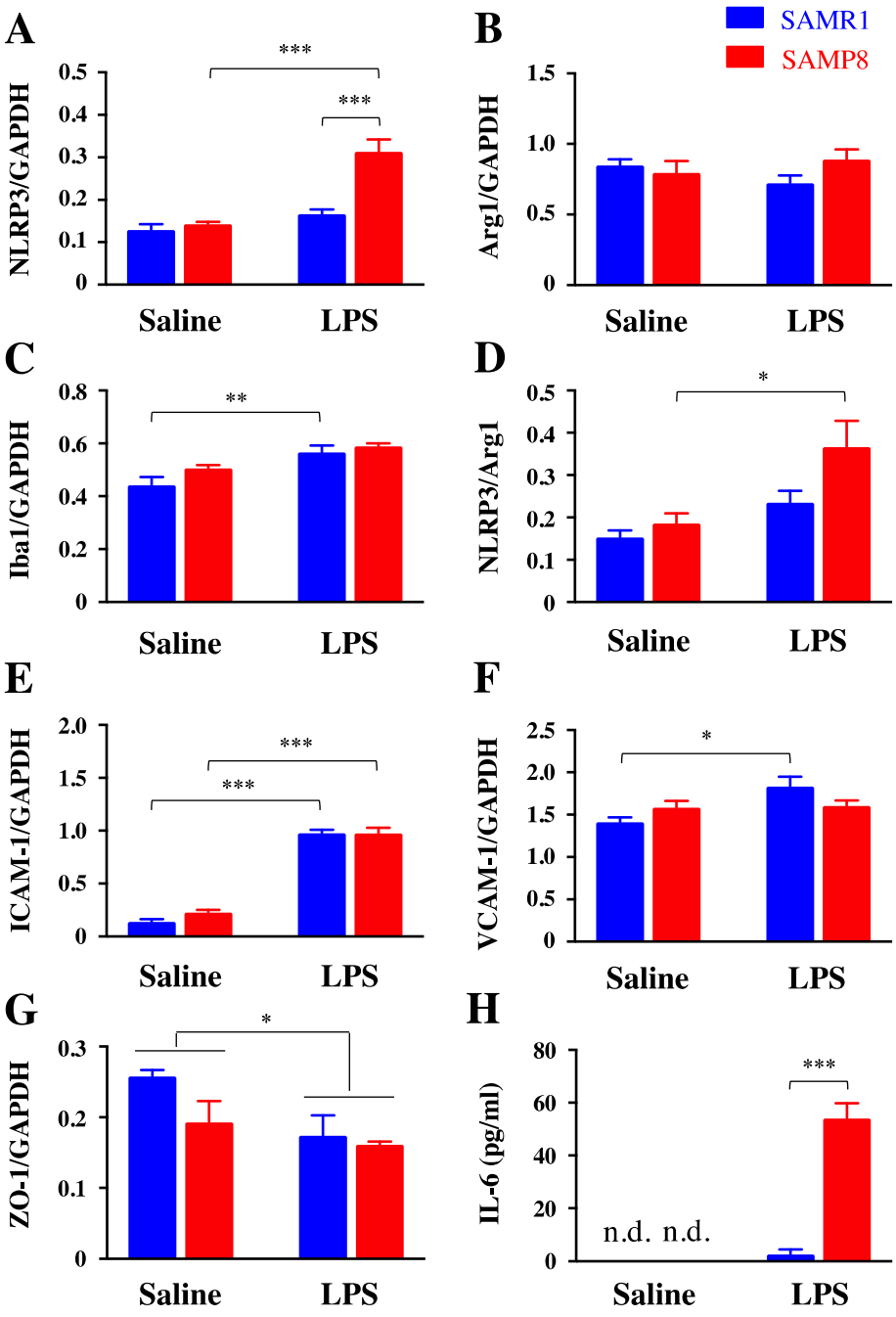


**Fig. 4.** LPS injection enhances neuroinflammation in SAMP8 mice. Brains and blood were collected 24 h post LPS injection from 17-week-old SAMR1 and SAMP8 mice. Proteins were extracted from coronal brain sections. The expression levels of proteins related to neuroinflammation (A–D), cell adhesion molecules (E, F), and a tight junction (G) were examined by western blot and normalized to GAPDH or Arg1. (H) The serum IL-6 level in 17-week-old SAMR1 and SAMP8 mice. Data are shown as the mean ± the SEM ($n = 4$). *$p < 0.05$, **$p < 0.01$, and ***$p < 0.001$.

show depression-like behaviors.

### 3.4. SAMP8 mice exhibit a disrupted circadian rhythm with aging

At 8 weeks old, the cumulative activity in the dark phase was significantly higher than that in the light phase in both SAMR1 and SAMP8 mice [Fig. 7B, left; two-way ANOVA; interaction, $F(1,66) = 23.6$, $p < 0.0001$; strain, $F(1,66) = 2.973$, $p = 0.0893$; light/dark, $F(1,66) = 185$, $p < 0.0001$; Bonferroni's post hoc test, $p < 0.001$]. In the dark phase, the cumulative activity in SAMR1 mice was significantly higher than that in SAMP8 mice ($p < 0.001$). Likewise, the average body temperature in the dark phase was significantly higher than that in the light phase in both SAMR1 and SAMP8 mice [Fig. 7B, right; two-way ANOVA; interaction, $F(1,66) = 6.642$, $p = 0.0122$; strain, $F(1,66) = 25.74$, $p < 0.0001$; light/dark, $F(1,66) = 196.6$, $p < 0.0001$; Bonferroni's post hoc test, $p < 0.001$]. In the light phase, the average body temperature in SAMR1 mice was significantly lower than that in SAMP8 mice ($p < 0.001$). In contrast, no differences in cumulative activity or average body temperature in SAMP8 mice at 17 weeks were found between light and dark phases, although SAMR1 mice still had their significant differences [Fig. 7C; two-way ANOVA; interaction (activity), $F(1,48) = 21.3$, $p < 0.0001$; strain (activity), $F(1,48) = 0.6682$, $p < 0.4177$; light/dark (activity), $F(1,48) = 20.58$, $p < 0.0001$; interaction (body temperature), $F(1,48) = 28.36$,

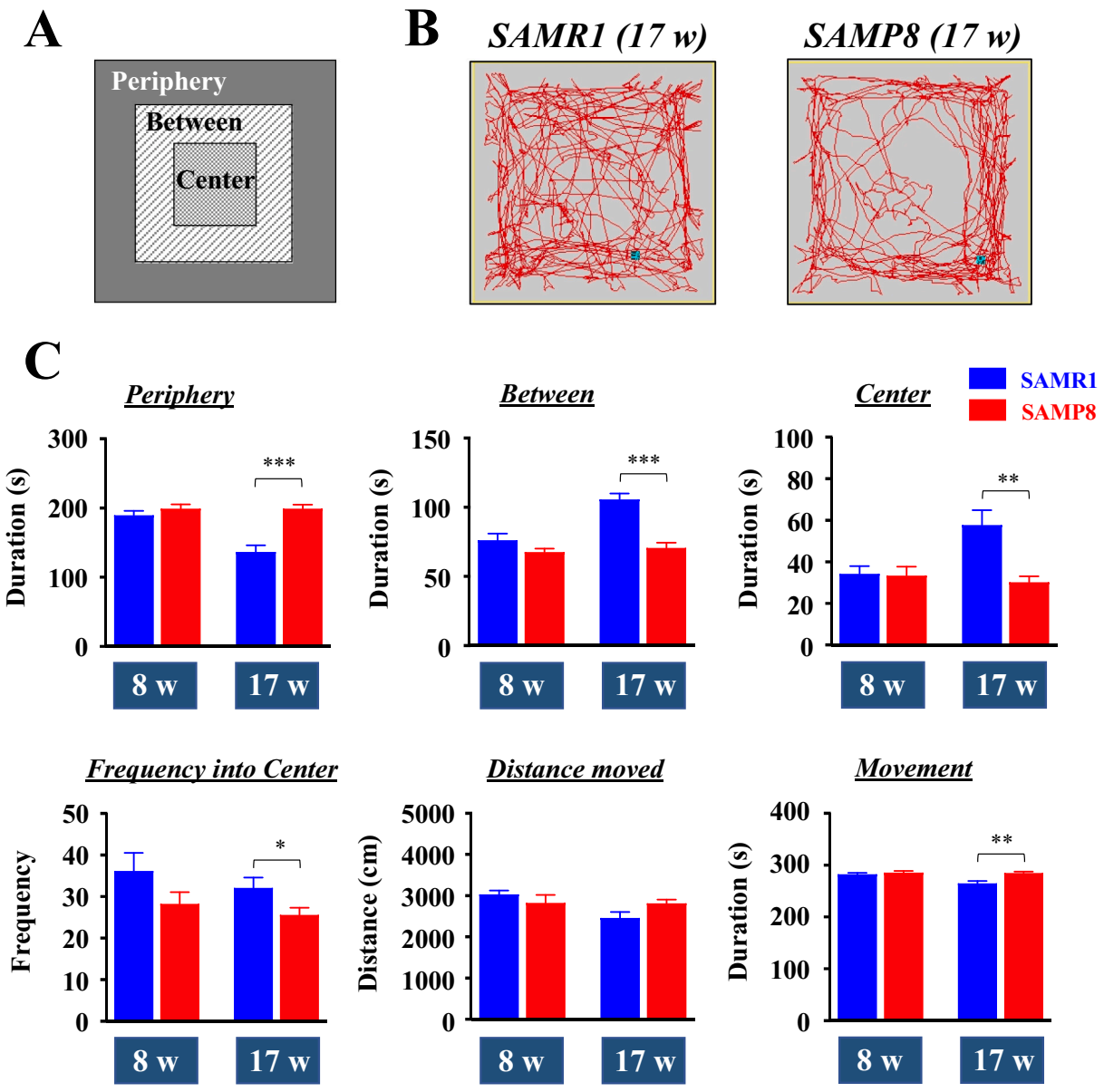


**Fig. 5.** SAMP8 mice show high anxiety levels with aging. (A) A schematic diagram showing 3 areas (center, between, and periphery) in an open field box (40 × 40 × 40 cm). (B) Representative 5-min tracking data of 17-week-old SAMR1 and SAMP8 mice in the OFT under the high light condition (120–130 lx). (C) Time spent in each area, frequency into the center, total distance moved, and total movement of SAMR1 and SAMP8 mice aged 8 and 17 weeks for 5 min in the OFT. Data are shown as the mean ± the SEM (8 w, $n = 8$; 17 w, $n = 13$). *$p < 0.05$, **$p < 0.01$, and ***$p < 0.001$. w, weeks of age.

$p < 0.0001$; strain (body temperature), $F(1,48) = 3.14$, $p < 0.0827$; light/dark (body temperature), $F(1,48) = 52.22$, $p < 0.0001$; Bonferroni's post hoc test, $p < 0.001$]. Notably, in the light phase, the cumulative activity and average body temperature in SAMP8 mice were significantly higher than those in SAMR1 mice ($p < 0.001$). These results suggest a circadian rhythm disruption in SAMP8 mice at 17 weeks.

## 4. Discussion

In this study, we found for the first time that SAMP8 mice had a brain microenvironment prone to neuroinflammatory priming at a relatively young age (17 weeks), but not 8 weeks (Fig. 8). It is plausible that this may lead to the emergence of anxiety- and depression-like behaviors and circadian rhythm disruption in SAMP8 mice. These findings highlight that neuroinflammatory priming, but not overt neuroinflammation, could underlie emotional disturbances in SAMP8 mice with aging.

Microglia, yolk-sac precursors-derived resident immune cells in the brain (Salter and Stevens, 2017), are key players for neuroinflammation; their activation could be a determinant for the onset of depression. Similarly, astroglial activation is involved in neuroinflammation (Ahmad et al., 2019). A notable finding has been reported that microglial activation precedes induction of reactive astrocytes (Liddelow et al., 2017). Hence, this study focused on the role of microglia in neuroinflammation in SAMP8 mice. Inflammatory responses were observed in microglia from the brains of SAMP8 mice at 17 weeks, but not 8 weeks, suggesting that microglial activation in response to LPS could be enhanced in SAMP8 mice with aging. This result is also likely to be consistent with previous findings showing that aged rodents sensitized microglial activation to ex vivo LPS challenges (Frank et al., 2010). On the other hand, under physiological conditions, no differences in the protein expression of proinflammatory (NLRP3) and anti-inflammatory (Arg1) factors were found in microglia isolated from the brains of SAMP8 mice aged 17 weeks. There was also no large difference in the

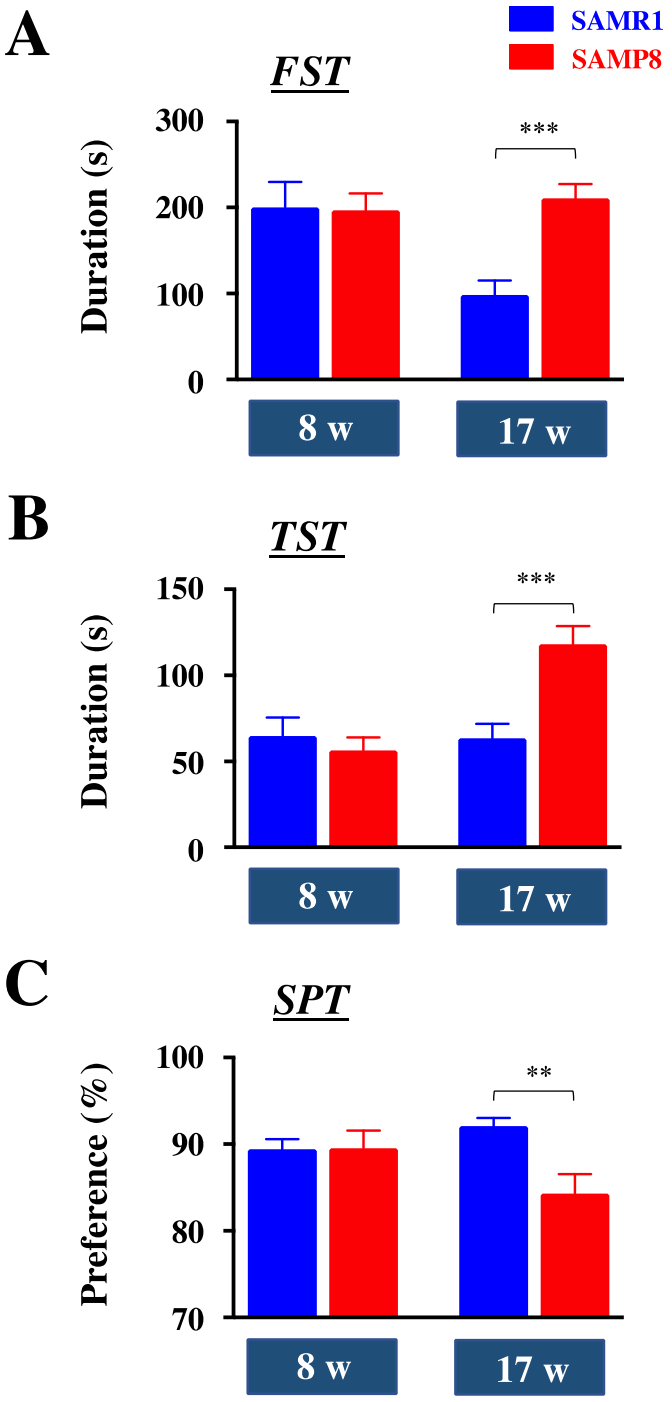


**Fig. 6.** SAMP8 mice exhibit depressive-like behaviors with aging. Depressive-like behaviors were examined by 3 different types of behavioral tests such as FST, TST, and SPT in SAMR1 and SAMP8 mice aged 8 and 17 weeks. The total duration of immobility during the last 4 min of the FST (A) or TST (B) for 6 min was scored. (C) The percentage of sucrose preference was assessed by the SPT. Data are shown as the mean ± the SEM [A (8 w, $n = 8$; 17 w, $n = 15$–16), B (8 w, $n = 8$; 17 w, $n = 14$), C (8 w, $n = 8$; 17 w, $n = 8$)]. $^{**}p < 0.01$ and $^{***}p < 0.001$. w, weeks of age.

proportion of pro- and anti-inflammatory phenotypes (NLRP3/Arg1) and brain cytokine levels between SAMR1 and SAMP8 mice of the same age, although a significant increase in brain cytokine levels was found at 41 weeks (Fig. S4). These results suggest that obvious and intense neuroinflammation is not observed in the brains of SAMP8 mice at 17 weeks.

Interestingly, increased expression of Cav2.2, an N-type voltage-dependent calcium channel, was found in microglia isolated from the brains of SAMP8 mice at 17 weeks. Given a recent study showing that microglial Cav2.2 plays a critical role in neuroinflammaging (Huntula et al., 2019), it would imply that elevated Cav2.2 levels in microglia underlie age-related neuroinflammatory priming in SAMP8 mice. In addition, 17-week-old SAMP8 mice showed an increase and a decrease in brain ICAM-1 and ZO-1 expression, respectively. ICAM-1, a cell adhesion molecule known to participate in brain neuroinflammation, recruits peripherally derived monocytes to the brain (Sawicki et al., 2015). ZO-1 is an endothelial tight junction protein expressed in microvessels that constitute the blood-brain-barrier (BBB) and regulates its permeability in the brain (Nico et al., 1999). Diminished tight junctions also induces a leaky BBB that could, in turn, lead to brain neuroinflammation by the infiltration of peripheral immune cells and cytokines (Sil et al., 2016). These findings along with our results indicate that SAMP8 mice would exhibit a brain microenvironment in which it is easier to trigger neuroinflammation during aging.

It has been reported that high levels of soluble ICAM-1, a circulating form of ICAM-1 in the blood and cerebrospinal fluid (Ramos et al., 2014), was found in elderly patients with depression (Thomas et al., 2007; van Agtmaal et al., 2017). This implies that soluble ICAM-1 is likely a biomarker candidate for late-life depression (Gregory et al., 2019). Therefore, future studies on soluble ICAM-1 levels in SAMP8 mice would be helpful to corroborate a link between neuroinflammation and depression during aging.

Furthermore, the present study using BMVEC cultures demonstrated LPS-induced enhancement of ICAM-1 and VCAM-1 expression, and LPS injection also showed an increase in pro-inflammatory states, as demonstrated by the elevated NLRP3 expression and increased ratio of NLRP3/Arg1 in the brain of SAMP8 mice at 17 weeks. Notably, high levels of plasma CORT in SAMP8 mice at 17 weeks could lead to a state that facilitates neuroinflammation, as supported by several studies showing that prior CORT exposure enhances the neuroinflammatory response to subsequent immunological stimulants such as LPS (Kelly et al., 2018; Smyth et al., 2004). Therefore, these results implicate that the brain microenvironment of SAMP8 mice shows a state of neuroinflammatory priming with aging, presumably through CORT effects. Intriguingly, significant elevation of serum IL-6 levels was found in LPS-injected SAMP8 mice, possibly suggesting that SAMP8 mice have a predisposition toward systemic inflammation as well as neuroinflammaging. This may also lead to vulnerable tight junctions of the BBB in SAMP8 mice, as supported by a finding showing an association of systemic inflammation with a disrupted BBB during aging (Elahy et al., 2015).

A battery of behavioral tests showed anxiety- and depression-like behaviors and behavioral circadian rhythm disruptions in SAMP8 mice at 17 weeks, but not 8 weeks. These results are consistent with previous findings using SAMP8 mice at similar ages (Yanai and Endo, 2016). Notably, onset of these behavioral changes likely requires neuroinflammatory priming, but does not require LPS challenges in SAMP8 mice. Further studies are needed to clarify how the priming state of neuroinflammaging could indeed trigger the mental disturbances.

It is of particular interest that the disrupted circadian rhythm of behavior and apathy as a depression-like behavior were already found in SAMP8 mice as early as 11 and 15 weeks of age, respectively (Fig. S6). It is well documented that the circadian rhythm is controlled by biological clock genes (Mohawk et al., 2012) and that its disruption is closely involved in the pathogenesis of psychiatric disorders including depression (Li et al., 2013; Vadnie and McClung, 2017) and aging (Nakamura et al., 2015; Tahara et al., 2017). Our preliminary data also suggest that there are some differences in the expression pattern of circadian clock genes between SAMR1 and SAMP8 mice as early as 8 weeks of age (data not shown). From the present results, the disruption of the behavioral circadian rhythm, presumably along with altered circadian clock gene expression, could precede the onset of depression-

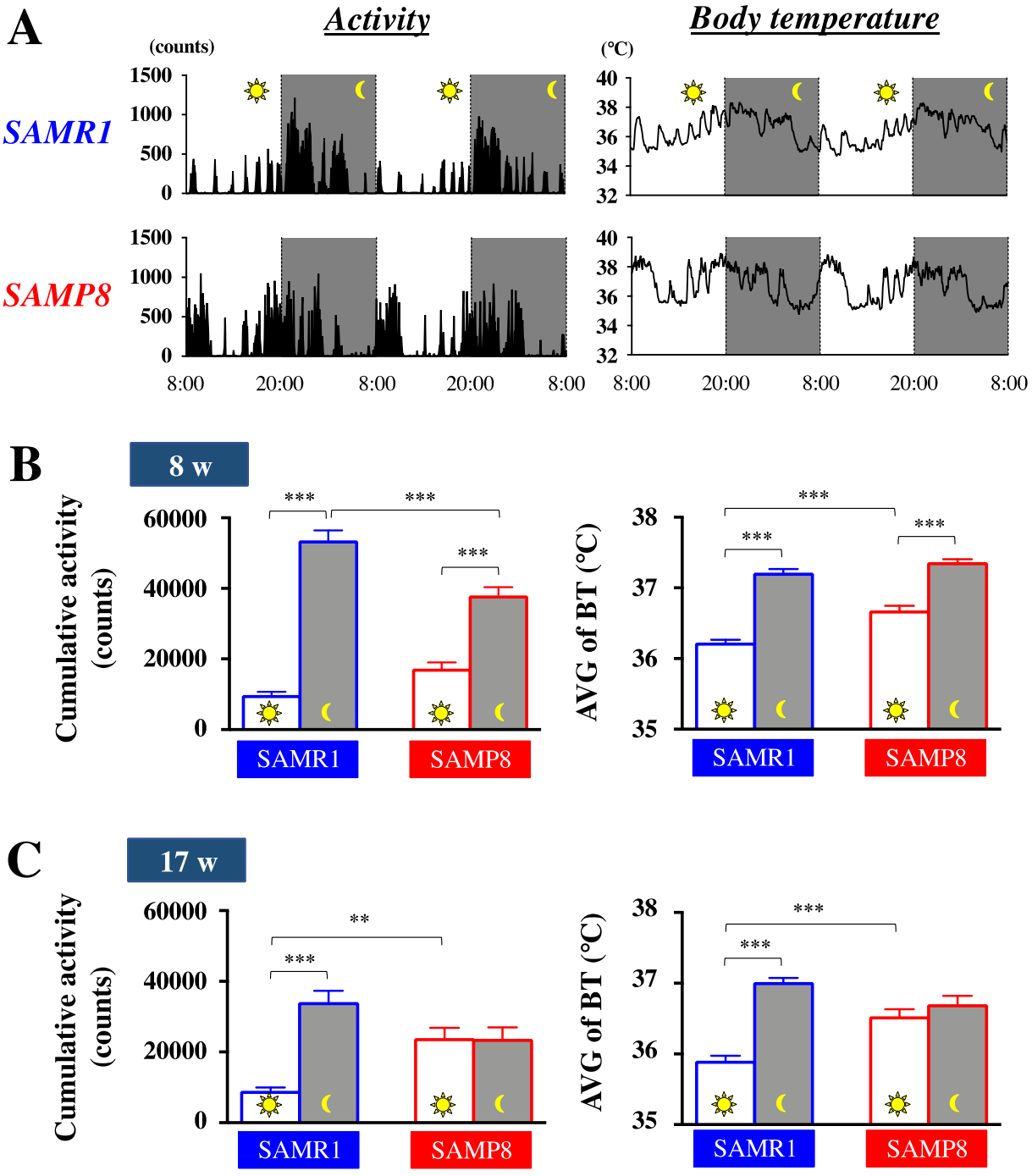


**Fig. 7.** The time course of locomotor activity and BT in home cages. (A) Representative actograms and changes in BT of SAMR1 and SAMP8 mice aged 17 weeks for 2 days. The time between 8:00 and 20:00 and between 20:00 and 8:00 indicates the diurnal (light) and nocturnal (dark) phases, respectively. The cumulative activity and average BT in the light and dark phases of SAMR1 and SAMP8 mice aged 8 (B) and 17 (C) weeks. Data are shown as the mean ± SEM [B (SAMR1, $n = 11$; SAMP8, $n = 24$), C (SAMR1, $n = 13$; SAMP8, $n = 13$)]. $^{**}p < 0.01$ and $^{***}p < 0.001$. w, weeks of age.

like behavior in SAMP8 mice, although it is not clear yet when neuroinflammation and anxiety-like behaviors are induced. Clarification of these relationships would need further intense research.

In addition, remarkable findings have been reported that the microglial neuroinflammatory response is also controlled by intrinsic clock genes (Fonken et al., 2015; Nakazato et al., 2017) and that the diminished circadian rhythm in microglia contributes to neuroinflammatory sensitization with aging (Fonken et al., 2016). These findings imply that neuroinflammaging in SAMP8 mice could be controlled by the microglial circadian clock.

In conclusion, the present study demonstrates that SAMP8 mice have a brain microenvironment in which it is easier to cause neuroinflammatory priming with aging. This could be also involved in behavioral deficits in emotion and circadian rhythms. These findings provide new insights into features of young SAMP8 mice regarding a close link between neuroinflammaging and behavioral alterations. This would aid to delving deeper into the understanding of pathophysiological mechanisms underlying emotional disturbances during aging. These findings also show that young SAMP8 mice can serve as an animal model of a pre-symptomatic state (e.g., pre-frailty state) for emotional disorders with aging and neuroinflammaging, providing an avenue for the development of therapeutic and preventive approaches

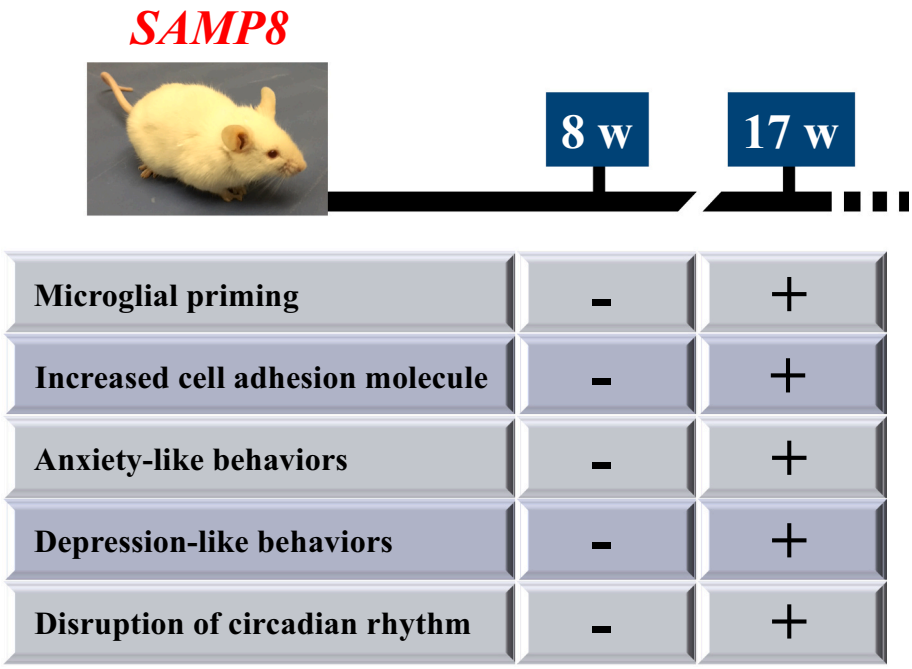


**Fig. 8.** A summary of neuroinflammatory priming and abnormal emotionality emerging with aging in SAMP8 mice. w, weeks of age.

to overcome age-related disorders.

## CRediT authorship contribution statement

**Naoki Ito**: Conceptualization, Formal analysis, Funding acquisition, Investigation, Methodology, Project administration, Validation, Visualization, Writing – original draft, Writing – review & editing. **Hiroaki Takemoto**: Formal analysis, Investigation, Methodology, Writing – review & editing. **Ayana Hasegawa**: Investigation. **Chika Sugiyama**: Investigation. **Kengo Honma**: Investigation. **Takayuki Nagai**: Supervision, Writing – review & editing. **Yoshinori Kobayashi**: Supervision, Writing – review & editing. **Hiroshi Odaguchi**: Funding acquisition, Project administration, Supervision, Writing – review & editing.

## Declaration of competing interest

The authors declare that they have no competing interests.

## Acknowledgements

We would like to thank Ms. Harumi Koguchi and Ms. Rina Fujita for their technical assistance. This work was supported by JSPS KAKENHI (Grant number 17K09320 to NI) and JST COI (Grant number JPMJCE1301 to NI and HO) grants. We also thank Editage (www.editage.p) for English language editing.

## Appendix A. Supplementary data

Supplementary data to this article can be found online at https://doi.org/10.1016/j.exger.2020.111109.

## References

Ahmad, M.H., Fatima, M., Mondal, A.C., 2019. Influence of microglia and astrocyte activation in the neuroinflammatory pathogenesis of Alzheimer's disease: rational insights for the therapeutic approaches. J. Clin. Neurosci. 59, 6–11.
Alexopoulos, G.S., 2019. Mechanisms and treatment of late-life depression. Transl. Psychiatry 9 (1), 188.
Banks, W.A., Coon, A.B., Robinson, S.M., Moinuddin, A., Shultz, J.M., Nakaoke, R., Morley, J.E., 2004. Triglycerides induce leptin resistance at the blood-brain barrier. Diabetes 53 (5), 1253–1260.
Carter, T.A., Greenhall, J.A., Yoshida, S., Fuchs, S., Helton, R., Swaroop, A., Lockhart, D.J., Barlow, C., 2005. Mechanisms of aging in senescence-accelerated mice. Genome Biol. 6 (6), R48.
Chen, G.H., Wang, C., Yangcheng, H.Y., Liu, R.Y., Zhou, J.N., 2007. Age-related changes in anxiety are task-specific in the senescence-accelerated prone mouse 8. Physiol. Behav. 91 (5), 644–651.
Chen, W., Liang, T., Zuo, W., Wu, X., Shen, Z., Wang, F., Li, C., Zheng, Y., Peng, G., 2018. Neuroprotective effect of 1-Deoxynojirimycin on cognitive impairment, beta-amyloid deposition, and neuroinflammation in the SAMP8 mice. Biomed Pharmacother 106, 92–97.
Cosin-Tomas, M., Alvarez-Lopez, M.J., Sanchez-Roige, S., Lalanza, J.F., Bayod, S., Sanfeliu, C., Pallas, M., Escorihuela, R.M., Kaliman, P., 2014. Epigenetic alterations in hippocampus of SAMP8 senescent mice and modulation by voluntary physical exercise. Front. Aging Neurosci. 6, 51.
Dalle, S., Rossmeislova, L., Koppo, K., 2017. The role of inflammation in age-related sarcopenia. Front. Physiol. 8, 1045.
de Magalhaes, J.P., 2013. How ageing processes influence cancer. Nat. Rev. Cancer 13 (5), 357–365.
Del Valle, J., Duran-Vilaregut, J., Manich, G., Casadesus, G., Smith, M.A., Camins, A., Pallas, M., Pelegri, C., Vilaplana, J., 2010. Early amyloid accumulation in the hippocampus of SAMP8 mice. J. Alzheimers Dis. 19 (4), 1303–1315.
Di Benedetto, S., Muller, L., Wenger, E., Duzel, S., Pawelec, G., 2017. Contribution of neuroinflammation and immunity to brain aging and the mitigating effects of physical and cognitive interventions. Neurosci. Biobehav. Rev. 75, 114–128.
Diaz-Perdigon, T., Belloch, F.B., Ricobaraza, A., Elboray, E.E., Suzuki, T., Tordera, R.M., Puerta, E., 2020. Early sirtuin 2 inhibition prevents age-related cognitive decline in a senescence-accelerated mouse model. Neuropsychopharmacology: official publication of the American College of Neuropsychopharmacology 45 (2), 347–357.
Dong, J., Liu, Y., Zhan, Z., Wang, X., 2018. MicroRNA-132 is associated with the cognition improvement following voluntary exercise in SAMP8 mice. Brain Res. Bull. 140, 80–87.
Elahy, M., Jackaman, C., Mamo, J.C., Lam, V., Dhaliwal, S.S., Giles, C., Nelson, D., Takechi, R., 2015. Blood-brain barrier dysfunction developed during normal aging is associated with inflammation and loss of tight junctions but not with leukocyte recruitment. Immun. Ageing 12, 2.
Fonken, L.K., Frank, M.G., Kitt, M.M., Barrientos, R.M., Watkins, L.R., Maier, S.F., 2015. Microglia inflammatory responses are controlled by an intrinsic circadian clock. Brain Behav. Immun. 45, 171–179.
Fonken, L.K., Kitt, M.M., Gaudet, A.D., Barrientos, R.M., Watkins, L.R., Maier, S.F., 2016. Diminished circadian rhythms in hippocampal microglia may contribute to age-related neuroinflammatory sensitization. Neurobiol. Aging 47, 102–112.
Franceschi, C., Bonafe, M., Valensin, S., Olivieri, F., De Luca, M., Ottaviani, E., De Benedictis, G., 2000. Inflamm-aging. An evolutionary perspective on immunosenescence. Ann. N. Y. Acad. Sci. 908, 244–254.
Frank, M.G., Barrientos, R.M., Watkins, L.R., Maier, S.F., 2010. Aging sensitizes rapidly isolated hippocampal microglia to LPS ex vivo. J. Neuroimmunol. 226 (1–2), 181–184.
Furman, D., Campisi, J., Verdin, E., Carrera-Bastos, P., Targ, S., Franceschi, C., Ferrucci, L., Gilroy, D.W., Fasano, A., Miller, G.W., Miller, A.H., Mantovani, A., Weyand, C.M., Barzilai, N., Goronzy, J.J., Rando, T.A., Effros, R.B., Lucia, A., Kleinstreuer, N., Slavich, G.M., 2019. Chronic inflammation in the etiology of disease across the life

span. Nat. Med. 25 (12), 1822–1832.
Gambino, C.M., Sasso, B.L., Bivona, G., Agnello, L., Ciaccio, M., 2019. Aging and neuroinflammatory disorders: New biomarkers and therapeutic targets. Curr. Pharm. Des. 25 (39), 4168–4174.
Gregory, M.A., Manuel-Apolinar, L., Sanchez-Garcia, S., Villa Romero, A.R., de Jesus Iuit Rivera, J., Basurto Acevedo, L., Grijalva-Otero, I., Cuadros-Moreno, J., Garcia-de la Torre, P., Guerrero Cantera, J., Garcia Dominguez, J.A., Martinez Gallardo, S., Vega Garcia, S., Mejia Alonso, L.A., Sanchez-Arenas, R., 2019. Soluble intercellular adhesion molecule-1 (sICAM-1) as a biomarker of vascular cognitive impairment in older adults. Dement. Geriatr. Cogn. Disord. 47 (4–6), 243–253.
Grinan-Ferre, C., Palomera-Avalos, V., Puigoriol-Illamola, D., Camins, A., Porquet, D., Pla, V., Aguado, F., Pallas, M., 2016. Behaviour and cognitive changes correlated with hippocampal neuroinflammaging and neuronal markers in female SAMP8, a model of accelerated senescence. Exp. Gerontol. 80, 57–69.
Grinan-Ferre, C., Corpas, R., Puigoriol-Illamola, D., Palomera-Avalos, V., Sanfeliu, C., Pallas, M., 2018. Understanding epigenetics in the neurodegeneration of Alzheimer's disease: SAMP8 mouse model. J. Alzheimers Dis. 62 (3), 943–963.
Gunasekaran, U., Gannon, M., 2011. Type 2 diabetes and the aging pancreatic beta cell. Aging 3 (6), 565–575.
Huntula, S., Saegusa, H., Wang, X., Zong, S., Tanabe, T., 2019. Involvement of N-type Ca (2+) channel in microglial activation and its implications to aging-induced exaggerated cytokine response. Cell Calcium 82, 102059.
Ito, N., Hirose, E., Ishida, T., Hori, A., Nagai, T., Kobayashi, Y., Kiyohara, H., Oikawa, T., Hanawa, T., Odaguchi, H., 2017. Kososan, a Kampo medicine, prevents a social avoidance behavior and attenuates neuroinflammation in socially defeated mice. J. Neuroinflammation 14 (1), 98.
Jiang, T., Yu, J.T., Zhu, X.C., Tan, M.S., Gu, L.Z., Zhang, Y.D., Tan, L., 2014. Triggering receptor expressed on myeloid cells 2 knockdown exacerbates aging-related neuroinflammation and cognitive deficiency in senescence-accelerated mouse prone 8 mice. Neurobiol. Aging 35 (6), 1243–1251.
Jiang, T., Xue, L.J., Yang, Y., Wang, Q.G., Xue, X., Ou, Z., Gao, Q., Shi, J.Q., Wu, L., Zhang, Y.D., 2018. AVE0991, a nonpeptide analogue of Ang-(1-7), attenuates aging-related neuroinflammation. Aging 10 (4), 645–657.
Kelly, K.A., Michalovicz, L.T., Miller, J.V., Castranova, V., Miller, D.B., O'Callaghan, J.P., 2018. Prior exposure to corticosterone markedly enhances and prolongs the neuroinflammatory response to systemic challenge with LPS. PLoS One 13 (1), e0190546.
Krishnan, V., Han, M.H., Graham, D.L., Berton, O., Renthal, W., Russo, S.J., Laplant, Q., Graham, A., Lutter, M., Lagace, D.C., Ghose, S., Reister, R., Tannous, P., Green, T.A., Neve, R.L., Chakravarty, S., Kumar, A., Eisch, A.J., Self, D.W., Lee, F.S., Tamminga, C.A., Cooper, D.C., Gershenfeld, H.K., Nestler, E.J., 2007. Molecular adaptations underlying susceptibility and resistance to social defeat in brain reward regions. Cell 131 (2), 391–404.
Landi, F., Calvani, R., Tosato, M., Martone, A.M., Ortolani, E., Savera, G., Sisto, A., Marzetti, E., 2016. Anorexia of aging: risk factors, consequences, and potential treatments. Nutrients 8 (2), 69.
Lee, J.K., Tansey, M.G., 2013. Microglia isolation from adult mouse brain. Methods Mol. Biol. 1041, 17–23.
Li, J.Z., Bunney, B.G., Meng, F., Hagenauer, M.H., Walsh, D.M., Vawter, M.P., Evans, S.J., Choudary, P.V., Cartagena, P., Barchas, J.D., Schatzberg, A.F., Jones, E.G., Myers, R.M., Watson Jr., S.J., Akil, H., Bunney, W.E., 2013. Circadian patterns of gene expression in the human brain and disruption in major depressive disorder. Proc. Natl. Acad. Sci. U. S. A. 110 (24), 9950–9955.
Liddelow, S.A., Guttenplan, K.A., Clarke, L.E., Bennett, F.C., Bohlen, C.J., Schirmer, L., Bennett, M.L., Munch, A.E., Chung, W.S., Peterson, T.C., Wilton, D.K., Frouin, A., Napier, B.A., Panicker, N., Kumar, M., Buckwalter, M.S., Rowitch, D.H., Dawson, V.L., Dawson, T.M., Stevens, B., Barres, B.A., 2017. Neurotoxic reactive astrocytes are induced by activated microglia. Nature 541 (7638), 481–487.
Lin, N., Pan, X.D., Chen, A.Q., Zhu, Y.G., Wu, M., Zhang, J., Chen, X.C., 2014. Tripchlorolide improves age-associated cognitive deficits by reversing hippocampal synaptic plasticity impairment and NMDA receptor dysfunction in SAMP8 mice. Behav. Brain Res. 258, 8–18.
Liu, M.Y., Yin, C.Y., Zhu, L.J., Zhu, X.H., Xu, C., Luo, C.X., Chen, H., Zhu, D.Y., Zhou, Q.G., 2018. Sucrose preference test for measurement of stress-induced anhedonia in mice. Nat. Protoc. 13 (7), 1686–1698.
Lopez-Otin, C., Blasco, M.A., Partridge, L., Serrano, M., Kroemer, G., 2013. The hallmarks of aging. Cell 153 (6), 1194–1217.
Markowska, A.L., Spangler, E.L., Ingram, D.K., 1998. Behavioral assessment of the senescence-accelerated mouse (SAM P8 and R1). Physiol. Behav. 64 (1), 15–26.
Meeker, H.C., Chadman, K.K., Heaney, A.T., Carp, R.I., 2013. Assessment of social interaction and anxiety-like behavior in senescence-accelerated-prone and -resistant mice. Physiol. Behav. 118, 97–102.
Mohawk, J.A., Green, C.B., Takahashi, J.S., 2012. Central and peripheral circadian clocks in mammals. Annu. Rev. Neurosci. 35, 445–462.
Nakamura, T.J., Nakamura, W., Tokuda, I.T., Ishikawa, T., Kudo, T., Colwell, C.S., Block, G.D., 2015. Age-related changes in the circadian system unmasked by constant conditions. eNeuro 2 (4).
Nakazato, R., Hotta, S., Yamada, D., Kou, M., Nakamura, S., Takahata, Y., Tei, H., Numano, R., Hida, A., Shimba, S., Mieda, M., Hinoi, E., Yoneda, Y., Takarada, T., 2017. The intrinsic microglial clock system regulates interleukin-6 expression. Glia 65 (1), 198–208.
Navone, S.E., Marfia, G., Invernici, G., Cristini, S., Nava, S., Balbi, S., Sangiorgi, S., Ciusani, E., Bosutti, A., Alessandri, G., Slevin, M., Parati, E.A., 2013. Isolation and expansion of human and mouse brain microvascular endothelial cells. Nat. Protoc. 8 (9), 1680–1693.
Nico, B., Quondamatteo, F., Herken, R., Marzullo, A., Corsi, P., Bertossi, M., Russo, G., Ribatti, D., Roncali, L., 1999. Developmental expression of ZO-1 antigen in the mouse blood-brain barrier. Brain Res. Dev. Brain Res. 114 (2), 161–169.
Pang, K.C., Miller, J.P., Fortress, A., McAuley, J.D., 2006. Age-related disruptions of circadian rhythm and memory in the senescence-accelerated mouse (SAMP8). Age (Dordr.) 28 (3), 283–296.
Papaconstantinou, J., 2019. The role of signaling pathways of inflammation and oxidative stress in development of senescence and aging phenotypes in cardiovascular disease. Cells 8 (11).
Perez-Caceres, D., Ciudad-Roberts, A., Rodrigo, M.T., Pubill, D., Camins, A., Camarasa, J., Escubedo, E., Pallas, M., 2013. Depression-like behavior is dependent on age in male SAMP8 mice. Biogerontology 14 (2), 165–176.
Pizza, V., Agresta, A., D'Acunto, C.W., Festa, M., Capasso, A., 2011. Neuroinflamm-aging and neurodegenerative diseases: an overview. CNS Neurol Disord Drug Targets 10 (5), 621–634.
Puigoriol-Illamola, D., Grinan-Ferre, C., Vasilopoulou, F., Leiva, R., Vazquez, S., Pallas, M., 2018. 11beta-HSD1 inhibition by RL-118 promotes autophagy and correlates with reduced oxidative stress and inflammation, enhancing cognitive performance in SAMP8 mouse model. Mol. Neurobiol. 55 (12), 8904–8915.
Ramos, T.N., Bullard, D.C., Barnum, S.R., 2014. ICAM-1: isoforms and phenotypes. J. Immunol. 192 (10), 4469–4474.
Salimi, S., Shardell, M.D., Seliger, S.L., Bandinelli, S., Guralnik, J.M., Ferrucci, L., 2018. Inflammation and trajectory of renal function in community-dwelling older adults. J. Am. Geriatr. Soc. 66 (4), 804–811.
Salter, M.W., Stevens, B., 2017. Microglia emerge as central players in brain disease. Nat. Med. 23 (9), 1018–1027.
Sanchez-Barcelo, E.J., Megias, M., Verduga, R., Crespo, D., 1997. Differences between the circadian system of two strains of senescence-accelerated mice (SAM). Physiol. Behav. 62 (6), 1225–1229.
Sawicki, C.M., McKim, D.B., Wohleb, E.S., Jarrett, B.L., Reader, B.F., Norden, D.M., Godbout, J.P., Sheridan, J.F., 2015. Social defeat promotes a reactive endothelium in a brain region-dependent manner with increased expression of key adhesion molecules, selectins and chemokines associated with the recruitment of myeloid cells to the brain. Neuroscience 302, 151–164.
Sil, S., Ghosh, A., Ghosh, T., 2016. Impairment of blood brain barrier is related with the neuroinflammation induced peripheral immune status in intracerebroventricular colchicine injected rats: an experimental study with mannitol. Brain Res. 1646, 278–286.
Singh, V., Mitra, S., Sharma, A.K., Gera, R., Ghosh, D., 2014. Isolation and characterization of microglia from adult mouse brain: selected applications for ex vivo evaluation of immunotoxicological alterations following in vivo xenobiotic exposure. Chem. Res. Toxicol. 27 (5), 895–903.
Smith, T.B., De Iuliis, G.N., Lord, T., Aitken, R.J., 2013. The senescence-accelerated mouse prone 8 as a model for oxidative stress and impaired DNA repair in the male germ line. Reproduction 146 (3), 253–262.
Smyth, G.P., Stapleton, P.P., Freeman, T.A., Concannon, E.M., Mestre, J.R., Duff, M., Maddali, S., Daly, J.M., 2004. Glucocorticoid pretreatment induces cytokine overexpression and nuclear factor-kappaB activation in macrophages. J. Surg. Res. 116 (2), 253–261.
Steru, L., Chermat, R., Thierry, B., Simon, P., 1985. The tail suspension test: a new method for screening antidepressants in mice. Psychopharmacology 85 (3), 367–370.
Tahara, Y., Takatsu, Y., Shiraishi, T., Kikuchi, Y., Yamazaki, M., Motohashi, H., Muto, A., Sasaki, H., Haraguchi, A., Kuriki, D., Nakamura, T.J., Shibata, S., 2017. Age-related circadian disorganization caused by sympathetic dysfunction in peripheral clock regulation. NPJ Aging Mech Dis 3, 16030.
Takeda, T., Hosokawa, M., Takeshita, S., Irino, M., Higuchi, K., Matsushita, T., Tomita, Y., Yasuhira, K., Hamamoto, H., Shimizu, K., Ishii, M., Yamamuro, T., 1981. A new murine model of accelerated senescence. Mech. Ageing Dev. 17 (2), 183–194.
Takeda, T., Hosokawa, M., Higuchi, K., 1997. Senescence-accelerated mouse (SAM): a novel murine model of senescence. Exp. Gerontol. 32 (1–2), 105–109.
Thomas, A.J., Morris, C., Davis, S., Jackson, E., Harrison, R., O'Brien, J.T., 2007. Soluble cell adhesion molecules in late-life depression. Int. Psychogeriatr. 19 (5), 914–920.
Tomobe, K., Nomura, Y., 2009. Neurochemistry, neuropathology, and heredity in SAMP8: a mouse model of senescence. Neurochem. Res. 34 (4), 660–669.
Vadnie, C.A., McClung, C.A., 2017. Circadian rhythm disturbances in mood disorders: insights into the role of the suprachiasmatic nucleus. Neural Plast 2017, 1504507.
van Agtmaal, M.J.M., Houben, A., Pouwer, F., Stehouwer, C.D.A., Schram, M.T., 2017. Association of microvascular dysfunction with late-life depression: a systematic review and meta-analysis. JAMA Psychiatry 74 (7), 729–739.
Watanabe, T., Dohgu, S., Takata, F., Nishioku, T., Nakashima, A., Futagami, K., Yamauchi, A., Kataoka, Y., 2013. Paracellular barrier and tight junction protein expression in the immortalized brain endothelial cell lines bEND.3, bEND.5 and mouse brain endothelial cell 4. Biol. Pharm. Bull. 36 (3), 492–495.
Woelfer, M., Kasties, V., Kahlfuss, S., Walter, M., 2019. The role of depressive subtypes within the neuroinflammation hypothesis of major depressive disorder. Neuroscience 403, 93–110.
Yanai, S., Endo, S., 2016. Early onset of behavioral alterations in senescence-accelerated mouse prone 8 (SAMP8). Behav. Brain Res. 308, 187–195.
Yanai, S., Toyohara, J., Ishiwata, K., Ito, H., Endo, S., 2017. Long-term cilostazol administration ameliorates memory decline in senescence-accelerated mouse prone 8 (SAMP8) through a dual effect on cAMP and blood-brain barrier. Neuropharmacology 116, 247–259.
Yirmiya, R., Rimmerman, N., Reshef, R., 2015. Depression as a microglial disease. Trends Neurosci. 38 (10), 637–658.
Zanker, J., Duque, G., 2019. Osteoporosis in older persons: old and new players. J. Am. Geriatr. Soc. 67 (4), 831–840.
Zhang, X., Li, G., Guo, L., Nie, K., Jia, Y., Zhao, L., Yu, J., 2013. Age-related alteration in cerebral blood flow and energy failure is correlated with cognitive impairment in the senescence-accelerated prone mouse strain 8 (SAMP8). Neurol. Sci. 34 (11), 1917–1924.